A Three-Band Substrate Integrated Waveguide Leaky-Wave Antenna Based on Composite Right/Left-Handed Structure

Seyed Sasan Haghighi, Abbas-Ali Heidari, and Masoud Movahhedi

***Abstract*—In this communication, the design and implementation of a three-band substrate integrated waveguide (SIW) leaky-wave antenna (LWA) based on the composite right/left-handed (CRLH) structure is presented. CRLH unit cell of the proposed antenna is composed of two adjacent interdigital slots with two vias between them. Two CRLH bands along with a new right-handed (RH) band between them are achieved through this structure. The first CRLH band (7.1–10.75 GHz) is balanced and the second one (15.1–21.75 GHz) is unbalanced with 0.25-GHz stop band. Beam scan angle in the first CRLH band is from -78° to $+78^\circ$, in the second one from -40° to $+20^\circ$ and in the new RH band (12.6–13.4 GHz) from $+22^\circ$ to $+54^\circ$. Antenna radiation efficiency in the first CRLH band is about 90%. Simulated and measured results are compared and there is a good agreement between them.**

***Index Terms*—Composite right/left-handed transmission line (CRLH TL), leaky-wave antenna (LWA), substrate integrated waveguide (SIW), three-band.**

I. Introduction

Recently, leaky-wave antennas (LWAs) are increasingly being used in radar and scanning systems. The LWA beam scans the space using frequency variations, which plays an important role in scanning applications [1].

One of the suitable structures to implement LWAs with capability of simple integration, high-power handling, and good isolation is the substrate integrated waveguide (SIW) structure [2]. Different LWAs based on SIW structure with different and interest properties have been proposed and used [4]–[11]. Two types of uniform LWAs with low and controllable sidelobe level were designed using meandering long slots on the broadside of a straight SIW section, and a straight long slot on the broadside of a meandering SIW section [4]. In [5] and [6], two LWAs were proposed with rectangular transverse slots (with linear polarization) and H-shaped slots (with circular polarization) on the top of SIW, respectively; these have narrow beamwidth and wide impedance bandwidth and their beam scanning range is from broadside to back-fire. The LWAs can also be designed by using partially reflective surfaces (PRS) on the side walls of SIW [7], [8]. An LWA was proposed in the millimeter-wave band with TE_{10} and TE_{20} modes by placing via-holes on the SIW sidewalls [9]. Nonuniform transverse slots were used to reduce sidelobe level and to improve radiation efficiency of the antenna in [10]. In [11], an LWA based on nonuniform slots with a butterfly-like arrangement was designed to obtain a high gain and low sidelobe level.

To expand the ability of LWAs' angle scanning within the ranges from back-fire to end-fire, composite right/left-handed transmission lines (CRLH TLs) have been recently proposed and used [3], [12]–[20]. By placing interdigital slots as series capacitor on CRLH cell, based on SIW and half-mode SIW (HMSIW) transmission lines, four types of LWAs were obtained with double-sided and one-sided radiation patterns [12]. In [13], a CRLH LWA with flexible polarization was suggested that six different polarizations, including four linear polarization cases and two circular polarization ones, were created. It consists of two symmetrical SIW lines (with two individual inputs) loaded with series interdigital capacitors with orthogonal 45 linearly polarized waves. In [14], a miniaturized CRLH LWA based on HMSIW was presented with circular polarization using ramp-shaped slots. A CRLH antenna was proposed in [15] to improve its bore-sight radiation bandwidth with two leaky-wave radiator elements which were located in different unit cells. A multilayered CRLH LWA was presented to design an LWA with a constant gain over the frequency bandwidth of the antenna [16]. In order to achieve low sidelobe level, an LWA was proposed using periodic longitudinal slots onto CRLH ridge SIW [17].

Recently, multiband CRLH LWAs have been widely taken into account [18]–[20]. A dual-band LWA was designed with dual periodic CRLH cells, which has an unbalanced CRLH band and a right-handed (RH) band [18]. Also, in [19], a dual-band LWA with two balanced CRLH bands were presented. This antenna, with one main beam in two CRLH bands, scans from back-fire to end-fire. An LWA based on extended-CRLH TLs was presented in [20], which has two balanced CRLH bands with a wide scanning range and controllable filtering capability.

In this communication, a novel three-band LWA based on CRLH transmission line using SIW structure is proposed. In our design, two CRLH bands (the first band is balanced and the second one is unbalanced with 0.25-GHz stopband) and a new RH band between them are obtained. The unit cell of the proposed LWA consists of two adjacent interdigital slots and four vias (two vias in the middle of the cell between the two slots and two vias at the end side of the cell). The antenna is composed of 20 unit cells and is fabricated on the standard single-layer PCB.

II. Proposed Structure

In this section, structure of the proposed three-band CRLH LWA will be explained. The antenna is designed and fabricated on the Rogers RT/duriod 5870 substrate with a permittivity of 2.33, a loss tangent of 0.0012, and a thickness of 0.787 mm.

A. CRLH Unit Cell

Structure of the CRLH unit cell of the proposed LWA is shown in Fig. 1. As seen, the unit cell contains two adjacent interdigital slots etched on the SIW surface. The main idea in the design of the structure that results in two CRLH bands comes from using of two interdigital slots in a CRLH unit cell. In fact, in such a case, each CRLH unit cell of the proposed structure is built from two conventional CRLH cells with different periods which will be repeated double periodically. Moreover, each of these unequal-period-CRLH cells creates its own frequency band. Generally, the idea of having two slots in each unit cell leads to two segregated CRLH bands. The optimum location of the slots in each cell will be set to achieve the minimum stop band between the LH and the RH regions at both CRLH bands. By reducing the distance between the slots, the stop band is reduced at each two CRLH bands. The conductor strip between two interdigital slots (on the center line of the cell) is connected to the ground plane with two vias. The distance between these vias is indicated by y_1 in Fig. 1. Moreover, two vias are placed at the end side of the cell which the distance

Manuscript received February 23, 2015; revised June 20, 2015; accepted July 06, 2015. Date of publication July 16, 2015; date of current version October 02, 2015.

The authors are with the Department of Electrical and Computer Engineering, Yazd University, Yazd 89195-741, Iran (e-mail: aheidari@yazd.ac.ir).

Color versions of one or more of the figures in this communication are available online at http://ieeexplore.ieee.org.

Digital Object Identifier 10.1109/TAP.2015.2456951

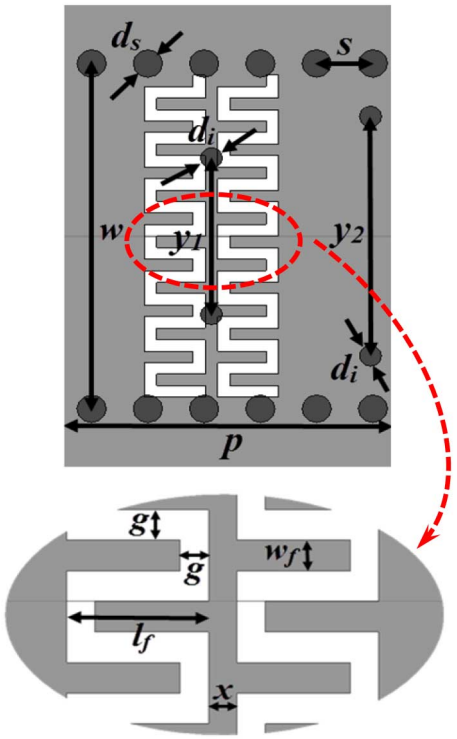

Fig. 1. Unit cell of the proposed SIW CRLH LWA.

between them is represented by y_2. Two interdigital slots generate series capacitance of the CRLH transmission line, while four internal vias together with SIW sidewall vias generate parallel inductance to form the equivalent circuit of the CRLH unit cell [3].

As seen in proposed structure in Fig. 1, in each unit cell, two interdigital slots are used to achieve two CRLH bands. These two CRLH bands are typically unbalanced with a large stop band. To remove the stop band in the first CRLH band and to obtain a new RH band, two vias are placed between interdigital slots at the center line of the unit cell. Based on our simulations, these two vias have little effect on reducing the stop band in the second CRLH band. Therefore, two additional vias are inserted at the end side of each cell. The insertion of these additional vias reduces the stop band in the second CRLH in addition to preserving balance condition in the first CRLH band. Furthermore, these vias can increase the frequency bandwidth of the new RH band.

B. Antenna Structure

The proposed CRLH LWA is composed of series connection of 20 CRLH unit cells presented in Fig. 1. Each side of this antenna is connected to a 50-Ω microstrip line through a tapered line for impedance matching. Fig. 2 shows the tapered microstrip feed line. The microstrip lines are connected to SMA 50-Ω connectors to form the input and output ports of the antenna. Increasing the number of cells to more than 20 cells has a negligible influence on the radiation efficiency and gain of the antenna in the three bands.

The antenna physical parameters that are shown in Figs. 1 and 2 and listed below were optimized for balance conditioning in the first CRLH band and also for minimizing the stop band in the second CRLH band. Cell length p should be chosen in a way that the CRLH bands are sufficiently close together and the RH band between them is not eliminated. Optimized antenna physical parameters (see Figs. 1 and 2) in millimeters are as follows: $w = 13.7$, $p = 11.8$, $d_s = 0.8$, $d_i = 0.5$, $s = 1.7$,

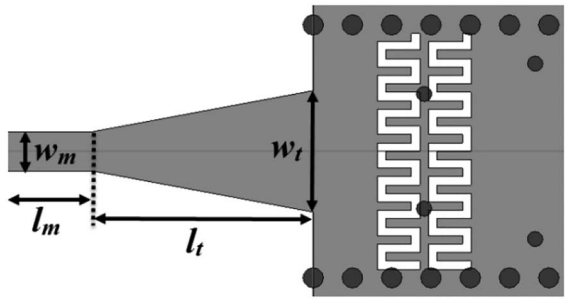

Fig. 2. Tapered microstrip feed line for impedance matching.

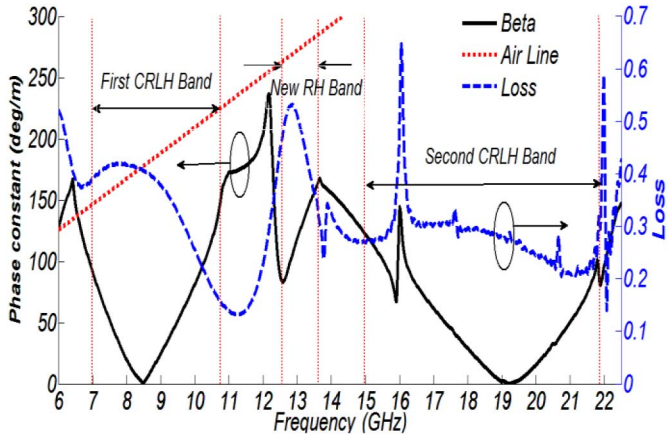

Fig. 3. Phase (β) and radiation loss of the proposed CRLH unit cell.

$g = 0.25$, $w_f = 0.25$, $x = 0.3$, $l_f = 2.1$, $y_1 = 6.8$, $y_2 = 10.7$, $w_t = 7.2$, $w_m = 2.3$, $l_t = 15$, and $l_m = 5$. The overall size of the antenna (including the ports) is 276 mm × 40 mm × 0.787 mm.

In Fig. 3, dispersion curve for the proposed CRLH unit cell (Fig. 1) is presented. In this figure, phase constant (β), radiation loss of the unit cell (including metal and dielectric losses), and the free-space wavenumber (k_0) are illustrated. Phase constant was extracted from the unit cell S-parameters, using driven mode simulation. In other words, to derive dispersion curve, the unit cell has been simulated in isolated configuration and hence mutual coupling between cells has been neglected. It should be stated that the radiation loss of the unit cell was determined by $\text{Loss} = 1 - |S11|^2 - |S21|^2$. As it can be seen in this figure, the LH (7.1–8.7 GHz) and RH (8.7–10.75 GHz) bands in the first CRLH band are continuous. However, in the second CRLH band, there is a stop band about 0.25 GHz between the LH (15–19 GHz) and RH (19.25–21.75 GHz) bands. Furthermore, a new RH band is generated between the first and second CRLH bands as marked in Fig. 3.

III. Simulation and Measurement Results

CST Microwave Studio commercial software was used for full-wave numerical simulations and optimization process [21]. The optimized LWA was fabricated for measurement validation of simulation results. Fig. 4 shows a photo of the fabricated antenna.

Fig. 5 shows the measured and simulated scattering parameters of the LW antenna. Agilent E8361C PNA Network Analyzer was used to measure the scattering parameters of the antenna. Considering Fig. 5(a), it is clear that the first CRLH band is from 7.1 to 10.75 GHz. Antenna beam at 8.7 GHz is toward the broadside. Simulation results in Figs. 3 and 5(a) reveal that the new RH band is from 12.6 to 13.4 GHz, while measured results indicate this band from 12.2 to

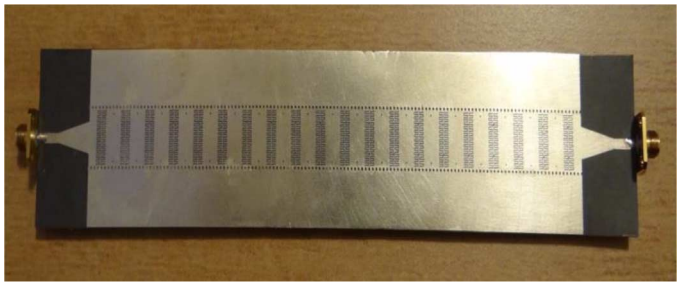

Fig. 4. Photograph of the fabricated antenna.

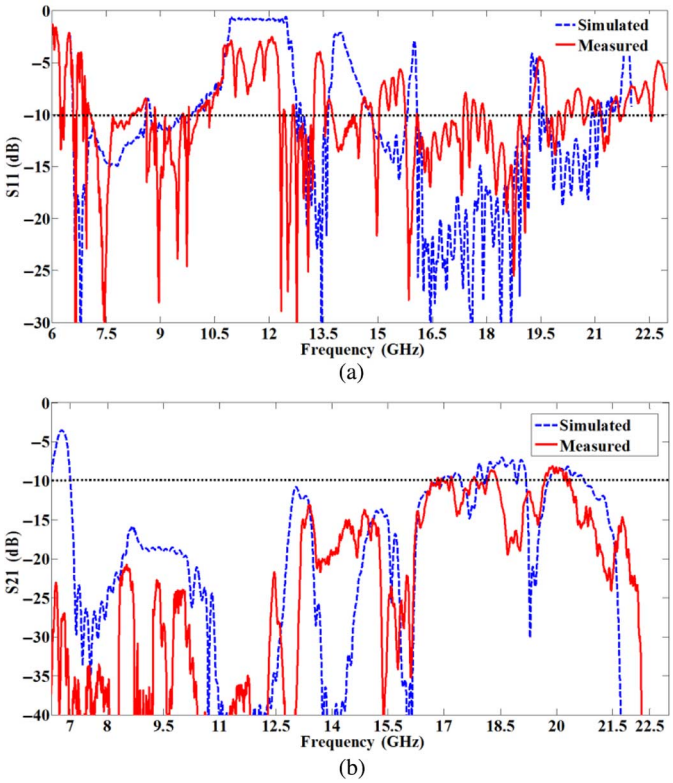

Fig. 5. Measured and simulated S-parameters of the antenna. (a) S_{11}. (b) S_{21}.

13.2 GHz. For the second CRLH band, simulation results reveal that LH region is from 15 to 19.2 GHz and RH region is from 19.45 to 21.75 GHz; but the measured results indicate that the LH region is from 14 to 19.2 GHz and RH region is from 19.6 to 22 GHz. Differences between the simulated and measured results are mainly due to manufacturing inaccuracies. As shown in Figs. 3 and 5, at the beginning of the second CRLH band in the LH region, there is a stop band due to the distance between two adjacent slots of each cell. The stop band is from 15.8 to 16.1 GHz in simulation and from 15 to 15.8 GHz in measurement. Furthermore, there is another stop band between LH and RH bands in the second CRLH band, due to unbalanced condition for the CRLH cell.

Simulated and measured antenna gains are shown in Fig. 6. The antenna gain increases by increasing frequency. By increasing frequency, difference between the measured and simulated gains becomes greater due to increasing sensitivity of manufacturing process and increasing losses in higher frequencies. The antenna measured gain in the first CRLH band at 8.7 GHz is about 13 dBi, in the new RH band at 13 GHz is 13.9 dBi, and in the second CRLH band at 19.1 GHz is approximately 15.1 dBi. Radiation efficiency of the antenna is

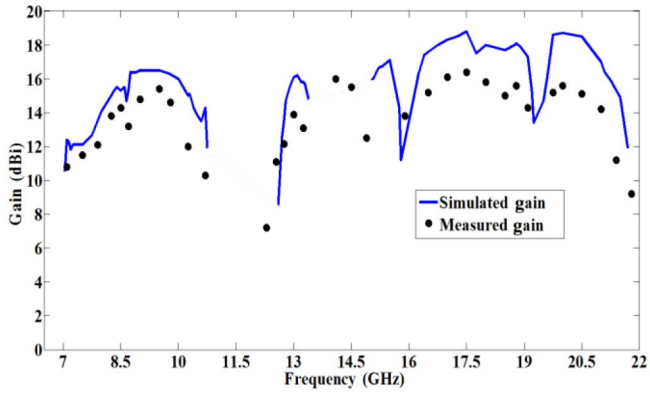

Fig. 6. Measured and simulated gains of the antenna.

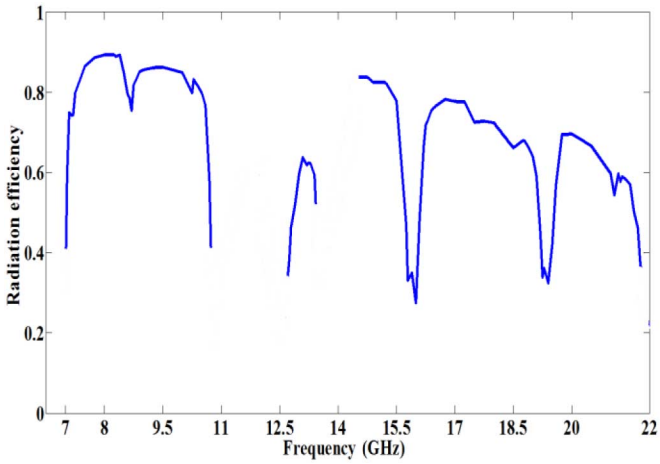

Fig. 7. Simulated radiation efficiency of the proposed LWA.

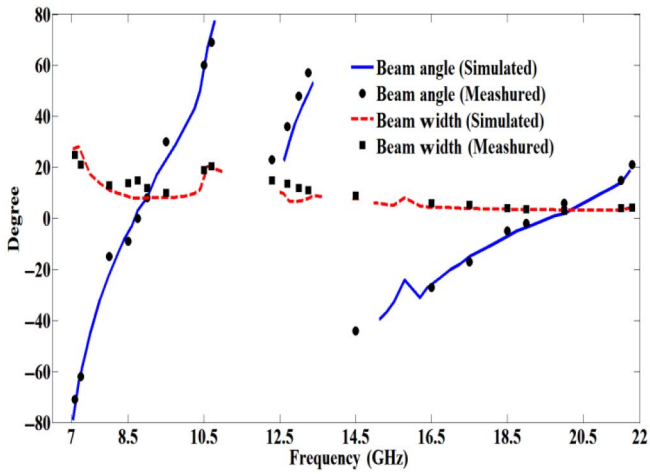

Fig. 8. Measured and simulated antenna beam angle and beamwidth.

displayed in Fig. 7. The antenna radiation efficiency is defined as the ratio of the total power radiated by an antenna to the net power accepted by the antenna from the connected transmitter and, in CST Microwave Studio software, is also defined as the ratio of the radiated power to accepted (input) power of the antenna [21]. The antenna radiation efficiency in the first CRLH band is about 90%, designating a good performance of the antenna in this band. Radiation efficiency of the new RH band is approximately 60% and is between 50% and 80%

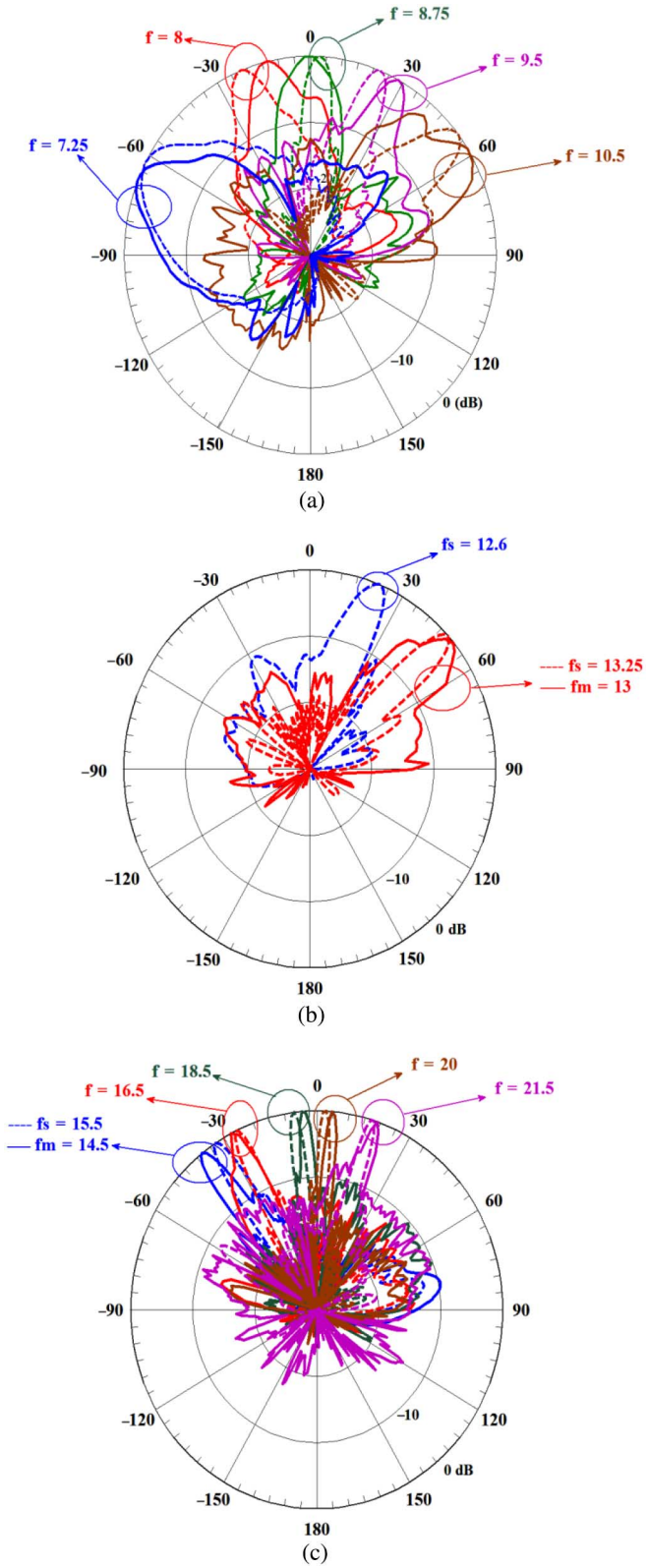

Fig. 9. Measured and simulated radiation patterns of the proposed antenna. Solid line: measurement results (fm). Dash line: simulation results (fs). (a) First CRLH band. (b) New RH band. (c) Second CRLH band.

for the second CRLH band. In the second CRLH band, radiation efficiency decreases by increasing frequency, because of increasing losses.

The beam scanning angle and 3-dB beamwidth have been shown in Fig. 8. In the first CRLH band, the antenna beam on the LH region starts from an angle of -78° and by increasing frequency in the RH region, it reaches to $+78^\circ$. For new RH band, beam scanning angle is from $+22^\circ$ to $+54^\circ$. In the second CRLH band, the antenna beam scans from -40° to -33° due to frequency increase from 15.1 to 15.8 GHz, from -31° to -1° due to frequency increase from 16.1 to 19.2 GHz, and from $+1^\circ$ to $+20^\circ$ for RH region. In the second CRLH band, due to the stop bands at the beginning of the LH region and between the LH and RH regions, antenna beam does not appear in angles from -31° to -33° and those from -1° to $+1^\circ$. The antenna half-power beamwidth varies from 7.5° to 12.5° in the first CRLH band and from 3.3° to 4.8° in the second CRLH band, and is about 7.5° in the new RH band. As shown in Fig. 8, by increasing the frequency, the antenna beamwidth is reduced.

TABLE I
COMPARISON OF THE PROPOSED ANTENNA AND THREE RECENTLY REPORTED MULTIBAND LWAS

	Ref. [18]	Ref. [19]	Ref. [20]	Our proposed antenna
Frequency bands	One unbalanced CRLH band + one new RH band	Two balanced CRLH band	Two balanced CRLH band	Two CRLH band+ new RH band
Maximum radiation efficiency	65%	Not reported	Not reported	90%
Scanning angle	CRLH band (100˚) , RH band (5˚)	First CRLH band (60˚), Second CRLH band (40˚)	First CRLH band (130˚), Second CRLH band (90˚)	First CRLH band (150˚), Second CRLH band (60˚) + RH band (34˚)

The simulated and measured normalized radiation patterns of the antenna are shown at a number of frequencies in the first CRLH band, in the new RH band, and in the second CRLH band in Fig. 9(a), (b), and (c), respectively. The simulated and measured sidelobe levels are less than -10 dB for all frequencies in Fig. 9. For the first CRLH band, new RH band, and LH region of the second CRLH band, cross polarization level is less than -20 dB, whereas for RH region of the second CRLH band, it is less than -12 dB.

Some features of our proposed antenna are compared with three recent proposed multiband LWAs in Table I. According to Table I and to the best of our knowledge, the proposed antenna in this communication is one of the first three-band CRLH LWAs. Also, the scan angle and radiation efficiency of the proposed antenna at the first CRLH band and the new RH band are greater than those in other references.

IV. CONCLUSION

A new three-band LWA based on CLRH SIW was proposed, optimized, and fabricated. The proposed LWA has two CRLH bands and a new RH band. The first CRLH band (balanced CRLH band) is from 7.05 to 10.75 GHz, the new RH band between the two CRLH bands is from 12.6 to 13.4 GHz, and the second CRLH band (unbalanced CRLH band with a 0.25-GHz stop band) is from 15.1 to 21.75 GHz. The antenna was designed using two adjacent interdigital slots in each CRLH cell, together with two vias between the slots. In order to reduce the stop-band in the second CRLH band, two vias were inserted at the end side of each cell. The antenna radiation beam scans from -78° to $+78^\circ$ in the first CRLH band, from $+22^\circ$ to $+54^\circ$ in the RH band, and from -40° to $+20^\circ$ in the second CRLH band. The maximum

measured gains of the antenna in the first CRLH band, the RH band, and the second CRLH band are 15.3, 16.1, and 17.3 dBi, respectively.

REFERENCES

[1] D. R. Jackson, A. A. Oliner, and C. Balanis, *Modern Antenna Handbook*. Hoboken, NJ, USA: Wiley, 2008.

[2] M. Bozzi, A. Georgiadis, and K. Wu, "Review of substrate integrated waveguide circuits and antennas," *IET Microw. Antennas Propag.*, vol. 5, no. 8, pp. 909–920, Jun. 2011.

[3] C. Caloz and T. Itoh, *Electromagnetic Metamaterials: Transmission Line Theory and Microwave Applications*. Hoboken, NJ, USA: Wiley, 2004.

[4] Y. J. Cheng, W. Hong, K. Wu, and Y. Fan, "Millimeter-wave substrate integrated waveguide long slot leaky-wave antennas and two-dimensional multi-beam applications," *IEEE Trans. Antennas Propag.*, vol. 59, no. 1, pp. 40–47, Jan. 2011.

[5] J. Liu, D. R. Jackson, and Y. Long, "Substrate integrated waveguide (SIW) leaky-wave antenna with transverse slots," *IEEE Trans. Antennas Propag.*, vol. 60, no. 1, pp. 20–29, Jan. 2012.

[6] J. Liu, X. Tang, and Y. Long, "Substrate integrated waveguide leaky wave antenna with H-shaped slots," *IEEE Trans. Antennas Propag.*, vol. 60, no. 8, pp. 3962–3967, Aug. 2012.

[7] A. J. Martinez-Ros, J. L. Gomez-Tornero, and G. Goussetis, "Holographic pattern synthesis with modulated substrate integrated waveguide line-source leaky-wave antennas," *IEEE Trans. Antennas Propag.*, vol. 61, no. 7, pp. 3466–3474, Jul. 2013.

[8] A. J. Martinez-Ros, J. L. Gomez-Tornero, and G. Goussetis, "Planar leaky-wave antenna with flexible control of the complex propagation constant," *IEEE Trans. Antennas Propag.*, vol. 60, no. 3, pp. 1625–1630, Mar. 2012.

[9] F. Xu, K. Wu, and X. Zhang, "Periodic leaky-wave antenna for millimeter wave applications based on substrate integrated waveguide," *IEEE Trans. Antennas Propag.*, vol. 58, no. 2, pp. 340–347, Feb. 2010.

[10] N. Gupta and V. D. Kumar, "Transverse non-uniform slotted substrate integrated waveguide leaky-wave antenna," in *Proc. IEEE Stud. Technol. Symp.*, Feb. 2014, pp. 138–142.

[11] Y. Mohtashami and J. Rashed-Mohassel, "A butterfly substrate integrated waveguide leaky-wave antenna," *IEEE Trans. Antennas Propag.*, vol. 62, no. 6, pp. 3384–3388, Jun. 2014.

[12] Y. Dong and T. Itoh, "Composite right/left-handed substrate integrated waveguide and half mode substrate integrated waveguide leaky-wave structures," *IEEE Trans. Antennas Propag.*, vol. 59, no. 3, pp. 767–775, Mar. 2011.

[13] Y. Dong and T. Itoh, "Substrate integrated composite right-/left-handed leaky-wave structure for polarization-flexible antenna application," *IEEE Trans. Antennas Propag.*, vol. 60, no. 2, pp. 760–771, Feb. 2012.

[14] A. P. Saghati, M. M. Mirsalehi, and M. H. Neshati, "A HMSIW circularly polarized leaky-wave antenna with backward, broadside, and forward radiation," *IEEE Antennas Wireless Propag. Lett.*, vol. 13, pp. 451–454, Mar. 2014.

[15] Nasimuddin, Z. N. Chen, and X. Qing, "Substrate integrated metamaterial-based leaky-wave antenna with improved bore-sight radiation bandwidth," *IEEE Trans. Antennas Propag.*, vol. 61, no. 7, pp. 3451–3457, Jul. 2013.

[16] Nasimuddin, Z. N. Chen, and X. Qing, "Multilayered composite right/left-handed leaky-wave antenna with consistent gain," *IEEE Trans. Antennas Propag.*, vol. 60, no. 11, pp. 5056–5062, Nov. 2012.

[17] Q. Yang, X. Zhao, and Y. Zhang, "Composite right/left-handed ridge substrate integrated waveguide slot array antennas," *IEEE Trans. Antennas Propag.*, vol. 62, no. 4, pp. 2311–2316, Apr. 2014.

[18] J. Cheng and A. Alphones, "Leaky-wave radiation behavior from a double periodic composite right/left handed substrate integrated waveguide," *IEEE Trans. Antennas Propag.*, vol. 60, no. 4, pp. 1727–1735, Apr. 2012.

[19] J. Machac, M. Polivka, and K. Zemlyakov, "A dual band leaky wave antenna on a CRLH substrate integrated waveguide," *IEEE Trans. Antennas Propag.*, vol. 61, no. 7, pp. 3876–3879, Jul. 2013.

[20] M. Duran-Sindreu, J. Choi, J. Bonache, F. Martin, and T. Itoh, "Dual-band leaky wave antenna with filtering capability based on extended-composite right/left-handed transmission lines," in *Proc. IEEE MTT-S Int. Microw. Symp. Dig.*, TH3F-3, pp. 1–4, Jun. 2013.

[21] CST Microwave Studio, version 2013, [Online]. Available: https://www.cst.com.

Space-Division Demultiplexing in Orbital-Angular-Momentum-Based MIMO Radio Systems

Matteo Oldoni, Fabio Spinello, Elettra Mari, Giuseppe Parisi, Carlo Giacomo Someda, Fabrizio Tamburini, Filippo Romanato, Roberto Antonio Ravanelli, Piero Coassini, and Bo Thidé

***Abstract*—Radio beams that carry nonzero orbital angular momentum (OAM) are analyzed from the viewpoint of a multiple-input-multiple-output (MIMO) communication system. Often, the natural OAM-beam orthogonality cannot be fully exploited because of spatial constraints on the receiving antenna size. Therefore, we investigate how far OAM-induced phase variations can be exploited in spatial demultiplexing based on conventional (linear momentum) receivers. Performances are investigated versus position and size of the transmitting and receiving devices. The use of OAM-mode coherent superpositions is also considered, in view of recent work by Edfors *et al.* Our final goal is to assess the merits of an OAM-based MIMO system, in comparison with a conventional one.**

***Index Terms*—Antenna spacing, multiple-input-multiple-output (MIMO), orbital angular momentum (OAM).**

I. INTRODUCTION

As the available radio spectrum becomes more and more crowded under the incessant strive for higher data-transfer capacities, several techniques have been, and currently are being, investigated, whose common aim is to increase the number of co-existing channels at a given frequency and over the same bandwidth. We will focus only on systems where transmitter (TX) and receiver (RX) are in line of sight (LOS), such as the typical back-haul links for mobile networks.

Polarization multiplexing is currently in wide use. It allows to double the available capacity by radiating and receiving fields with two orthogonal polarization states. More recently, multiple-input-multiple-output (MIMO) techniques have drawn attention for both short- and medium-distance applications. Although the mathematical theory of MIMO (i.e., [2] and [3]) holds for any system with more than one TX and/or RX (including polarization diversity), here we will use the acronym MIMO to refer to systems with antenna arrays on both TX and RX sides, with suitable pre- and postprocessing networks. Usually, such processing capabilities are adaptive, rely on channel estimation, and are typically implemented at the baseband digital stage. The theoretical increase in capacity offered by MIMO techniques is

Manuscript received January 20, 2015; revised July 06, 2015; accepted July 09, 2015. Date of publication July 16, 2015; date of current version October 02, 2015.

M. Oldoni, R. A. Ravanelli, and P. Coassini are with the R&D Department, SIAE Microelettronica, IT-20093 Cologno Monzese (MI), Italy (e-mail: matteo.oldoni@siaemic.com).

F. Spinello is with the Department of Information Engineering, Università di Padova, IT-35131, Padova, Italy, and also with TwistOff S.R.L., IT-35129 Padova, Italy.

E. Mari, G. Parisi, C. G. Someda, and F. Tamburini are with TwistOff S.R.L., IT-35129 Padova, Italy.

F. Romanato is with the Department of Physics and Astronomy "G. Galilei," Università di Padova, IT-35131 Padova, Italy.

B. Thidé is with the Ångstrom Laboratory, Swedish Institute of Space Physics, SE-75121 Uppsala, Sweden.

Color versions of one or more of the figures in this communication are available online at http://ieeexplore.ieee.org.

Digital Object Identifier 10.1109/TAP.2015.2456953